REFERENCES

1. Feinberg AP, Vogelstein B. Hypomethylation distinguishes genes of some human cancers from their normal counterparts. Nature. 6 (January 1983); 301(5895): 89-92.
2. Feinberg AP, Tycko B. The history of cancer epigenetics. Nat Rev Cancer. (February 2004); 4(2): 143-53.
3. Chalitchagorn K, Shuangshoti S, Hourpai N, Kongruttanachok N, Tangkijvanich P, Thong-ngam D, et al. Distinctive pattern of LINE-1 methylation level in normal tissues and the association with carcinogenesis. Oncogene. 18 (November 2004); 23(54): 8841-6.
4. Lengauer C, Kinzler KW, Vogelstein B. DNA methylation and genetic instability in colorectal cancer cells. Proc Natl Acad Sci U S A. 18 (March1997); 94(6): 2545-50.
5. Eden A, Gaudet F, Waghmare A, Jaenisch R. Chromosomal instability and tumors promoted by DNA hypomethylation. Science. 2003 Apr 18;300(5618):455.
6. Chen RZ, Pettersson U, Beard C, Jackson-Grusby L, Jaenisch R. DNA hypomethylation leads to elevated mutation rates. Nature. 3 (September 1998); 395(6697): 89-93.
7. Vilenchik MM, Knudson AG. Endogenous DNA double-strand breaks: production, fidelity of repair, and induction of cancer. Proc Natl Acad Sci U S A. 28 (October 2003); 100(22): 12871-6.
8. van Gent DC, Hoeijmakers JH, Kanaar R. Chromosomal stability and the DNA double-stranded break connection. Nat Rev Genet. (March 2001); 2(3): 196-206.
9. Mills KD, Ferguson DO, Alt FW. The role of DNA breaks in genomic instability and tumorigenesis. Immunol Rev. (August 2003);194: 77-95.
10. Valerie K, Povirk LF. Regulation and mechanisms of mammalian double-strand break repair. Oncogene. 1 (September 2003); 22(37): 5792-812.
11. Dasika GK, Lin SC, Zhao S, Sung P, Tomkinson A, Lee EY. DNA damage-induced cell cycle checkpoints and DNA strand break repair in development and tumorigenesis. Oncogene. 20 (December 1999); 18(55): 7883-99.

12. An J, Xu QZ, Sui JL, Bai B, Zhou PK. Downregulation of c-myc protein by siRNA-mediated silencing of DNA-PKcs in HeLa cells. Int J Cancer. 20 (November 2005); 117(4): 531-7.

13. Takata M, Sasaki MS, Sonoda E, Morrison C, Hashimoto M, Utsumi H, et al. Homologous recombination and non-homologous end-joining pathways of DNA double-strand break repair have overlapping roles in the maintenance of chromosomal integrity in vertebrate cells. Embo J. 15 (September 1998); 17(18): 5497-508.

14. Lengauer C, Kinzler KW, Vogelstein B. Genetic instabilities in human cancers. Nature. 17 (December 1998); 396(6712): 643-9.

15. Smith GC, Jackson SP. The DNA-dependent protein kinase. Genes Dev. 15 (April 1999); 13(8): 916-34.

16. Strathdee G, Brown R. Aberrant DNA methylation in cancer: potential clinical interventions. Expert Rev Mol Med. 4 (March 2002); 2002:1-17.

17. Robertson KD, Uzvolgyi E, Liang G, Talmadge C, Sumegi J, Gonzales FA, et al. The human DNA methyltransferases (DNMTs) 1, 3a and 3b: coordinate mRNA expression in normal tissues and overexpression in tumors. Nucleic Acids Res. 1 (June 1999); 27(11): 2291-8.

18. Dunn BK. Hypomethylation: one side of a larger picture. Ann N Y Acad Sci. (March 2003); 983: 28-42.

19. Costello JF, Plass C. Methylation matters. J Med Genet. (May 2001); 38(5): 285-303.

20. Schlissel M, Constantinescu A, Morrow T, Baxter M, Peng A. Double-strand signal sequence breaks in V(D)J recombination are blunt, 5'-phosphorylated, RAG-dependent, and cell cycle regulated. Genes Dev. (December 1993); 7(12B): 2520-32.

21. Papavasiliou FN, Schatz DG. Cell-cycle-regulated DNA double-stranded breaks in somatic hypermutation of immunoglobulin genes. Nature. 9 (November 2000); 408(6809): 216-21.

22. Nelson DL, Ledbetter SA, Corbo L, Victoria MF, Ramirez-Solis R, Webster TD, et al. Alu polymerase chain reaction: a method for rapid isolation of human-specific

sequences from complex DNA sources. Proc Natl Acad Sci U S A. (September 1989); 86(17): 6686-90.

23. Rogakou EP, Pilch DR, Orr AH, Ivanova VS, Bonner WM. DNA double-stranded breaks induce histone H2AX phosphorylation on serine 139. J Biol Chem. 6 (March 1998); 273(10): 5858-68.
24. Boyd KE, Farnham PJ. Coexamination of site-specific transcription factor binding and promoter activity in living cells. Mol Cell Biol. (December 1999); 19(12): 8393-9.
25. Fuks F. DNA methylation and histone modifications: teaming up to silence genes. Curr Opin Genet Dev. (October 2005); 15(5): 490-5.
26. Cameron EE, Bachman KE, Myohanen S, Herman JG, Baylin SB. Synergy of demethylation and histone deacetylase inhibition in the re-expression of genes silenced in cancer. Nat Genet. (January 1999); 21(1): 103-7.
27. Cahill DP, Kinzler KW, Vogelstein B, Lengauer C. Genetic instability and darwinian selection in tumours. Trends Cell Biol. (December 1999); 9(12): M57-60.
28. Breivik J. Don't stop for repairs in a war zone: Darwinian evolution unites genes and environment in cancer development. Proc Natl Acad Sci U S A. 8 (May 2001); 98(10): 5379-81.
29. Modrich P, Lahue R. Mismatch repair in replication fidelity, genetic recombination, and cancer biology. Annu Rev Biochem. (1996); 65: 101-33.
30. Ionov Y, Peinado MA, Malkhosyan S, Shibata D, Perucho M. Ubiquitous somatic mutations in simple repeated sequences reveal a new mechanism for colonic carcinogenesis. Nature. 10 (June 1993); 363(6429): 558-61.
31. Peinado MA, Malkhosyan S, Velazquez A, Perucho M. Isolation and characterization of allelic losses and gains in colorectal tumors by arbitrarily primed polymerase chain reaction. Proc Natl Acad Sci U S A. 1 (November 1992); 89(21): 10065-9.
32. Aaltonen LA, Peltomaki P, Leach FS, Sistonen P, Pylkkanen L, Mecklin JP, et al. Clues to the pathogenesis of familial colorectal cancer. Science. 7 (May 1993); 260(5109): 812-6.
33. Lynch HT, Lynch JF. 25 years of HNPCC. Anticancer Res. (July-August 1994); 14(4B): 1617-24.

34. Lynch HT, Smyrk TC. Identifying hereditary nonpolyposis colorectal cancer. N Engl J Med. 21 (May 1998); 338(21): 1537-8.

35. Lipkin SM, Wang V, Jacoby R, Banerjee-Basu S, Baxevanis AD, Lynch HT, et al. MLH3: a DNA mismatch repair gene associated with mammalian microsatellite instability. Nat Genet. (January 2000); 24(1): 27-35.

36. Jallepalli PV, Lengauer C. Chromosome segregation and cancer: cutting through the mystery. Nat Rev Cancer. (November 2001); 1(2): 109-17.

37. Jallepalli PV, Waizenegger IC, Bunz F, Langer S, Speicher MR, Peters JM, et al. Securin is required for chromosomal stability in human cells. Cell. 18 (May 2001); 105(4): 445-57.

38. Michel LS, Liberal V, Chatterjee A, Kirchwegger R, Pasche B, Gerald W, et al. MAD2 haplo-insufficiency causes premature anaphase and chromosome instability in mammalian cells. Nature. 18 (January 2001); 409(6818): 355-9.

39. Mohaghegh P, Hickson ID. Premature aging in RecQ helicase-deficient human syndromes. Int J Biochem Cell Biol. (November 2002); 34(11): 1496-501.

40. Khakhar RR, Cobb JA, Bjergbaek L, Hickson ID, Gasser SM. RecQ helicases: multiple roles in genome maintenance. Trends Cell Biol. (September 2003); 13(9): 493-501.

41. Narod SA, Foulkes WD. BRCA1 and BRCA2: 1994 and beyond. Nat Rev Cancer. (September 2004); 4(9): 665-76.

42. Venkitaraman AR. Cancer susceptibility and the functions of BRCA1 and BRCA2. Cell. 25 (January 2002); 108(2): 171-82.

43. Marx J. Debate surges over the origins of genomic defects in cancer. Science. 26 (July 2002); 297(5581): 544-6.

44. Adams JM, Harris AW, Pinkert CA, Corcoran LM, Alexander WS, Cory S, et al. The c-myc oncogene driven by immunoglobulin enhancers induces lymphoid malignancy in transgenic mice. Nature. 12-18 (December 1985); 318(6046): 533-8.

45. Adams JM, Harris AW, Langdon WY, Pinkert CA, Brinster RL, Palmiter RD, et al. c-myc-induced lymphomagenesis in transgenic mice and the role of the Pvt-1 locus in lymphoid neoplasia. Curr Top Microbiol Immunol. (1986); 132: 1-8.

46. Faderl S, Talpaz M, Estrov Z, O'Brien S, Kurzrock R, Kantarjian HM. The biology of chronic myeloid leukemia. N Engl J Med. 15 (July 1999); 341(3): 164-72.

47. Wong S, Witte ON. Modeling Philadelphia chromosome positive leukemias. Oncogene. 10 (September 2001); 20(40): 5644-59.

48.Hayashi Y. The molecular genetics of recurring chromosome abnormalities in acute myeloid leukemia. Semin Hematol. (October 2000); 37(4): 368-80.

49. Bartram CR. Molecular genetic aspects of myelodysplastic syndromes. Hematol Oncol Clin North Am. (June 1992); 6(3): 557-70.

50. Goelz SE, Vogelstein B, Hamilton SR, Feinberg AP. Hypomethylation of DNA from benign and malignant human colon neoplasms. Science. 12 (April 1985); 228(4696): 187-90.

51. Kaneda A, Tsukamoto T, Takamura-Enya T, Watanabe N, Kaminishi M, Sugimura T, et al. Frequent hypomethylation in multiple promoter CpG islands is associated with global hypomethylation, but not with frequent promoter hypermethylation. Cancer Sci. (January 2004); 95(1): 58-64.

52. Sugimura T. Cancer prevention: past, present, future. Mutat Res. 18 (June 1998); 402(1-2): 7-14.

53. Jurgens B, Schmitz-Drager BJ, Schulz WA. Hypomethylation of L1 LINE sequences prevailing in human urothelial carcinoma. Cancer Res. 15 (December 1996); 56(24): 5698-703.

54. Kazazian HH, Jr., Moran JV. The impact of L1 retrotransposons on the human genome. Nat Genet. (May 1998); 19(1): 19-24.

55. Florl AR, Lower R, Schmitz-Drager BJ, Schulz WA. DNA methylation and expression of LINE-1 and HERV-K provirus sequences in urothelial and renal cell carcinomas. Br J Cancer. (July 1999); 80(9): 1312-21.

56. Takai D, Yagi Y, Habib N, Sugimura T, Ushijima T. Hypomethylation of LINE1 retrotransposon in human hepatocellular carcinomas, but not in surrounding liver cirrhosis. Jpn J Clin Oncol. (July 2000); 30(7): 306-9.

57. Suter CM, Martin DI, Ward RL. Hypomethylation of L1 retrotransposons in colorectal cancer and adjacent normal tissue. Int J Colorectal Dis. (March 2004); 19(2): 95-101.

58. Santourlidis S, Florl A, Ackermann R, Wirtz HC, Schulz WA. High frequency of alterations in DNA methylation in adenocarcinoma of the prostate. Prostate. 15 (May 1999); 39(3): 166-74.

59. Xiong Z, Laird PW. COBRA: a sensitive and quantitative DNA methylation assay. Nucleic Acids Res. 15 (June 1997); 25(12): 2532-4.

60. Del Senno L, Maestri I, Piva R, Hanau S, Reggiani A, Romano A, et al. Differential hypomethylation of the c-myc protooncogene in bladder cancers at different stages and grades. J Urol. (July 1989); 142(1): 146-9.

61. Vachtenheim J, Horakova I, Novotna H. Hypomethylation of CCGG sites in the 3' region of H-ras protooncogene is frequent and is associated with H-ras allele loss in non-small cell lung cancer. Cancer Res. 1 (March 1994); 54(5): 1145-8.

62. Guo Y, Pakneshan P, Gladu J, Slack A, Szyf M, Rabbani SA. Regulation of DNA methylation in human breast cancer. Effect on the urokinase-type plasminogen activator gene production and tumor invasion. J Biol Chem. 1 (November 2002); 277(44): 41571-9.

63. Ostertag EM, Kazazian HH, Jr. Biology of mammalian L1 retrotransposons. Annu Rev Genet. (2001); 35: 501-38.

64. Martin SL, Branciforte D. Synchronous expression of LINE-1 RNA and protein in mouse embryonal carcinoma cells. Mol Cell Biol. (September 1993); 13(9): 5383-92.

65. Bratthauer GL, Fanning TG. Active LINE-1 retrotransposons in human testicular cancer. Oncogene. (March 1992); 7(3): 507-10.

66. Staley K, Blaschke AJ, Chun J. Apoptotic DNA fragmentation is detected by a semi-quantitative ligation-mediated PCR of blunt DNA ends. Cell Death Differ. (January 1997); 4(1): 66-75.

67. Xu GL, Bestor TH, Bourc'his D, Hsieh CL, Tommerup N, Bugge M, et al. Chromosome instability and immunodeficiency syndrome caused by mutations in a DNA methyltransferase gene. Nature. 11 (November 1999); 402(6758): 187-91.

68. Jeanpierre M, Turleau C, Aurias A, Prieur M, Ledeist F, Fischer A, et al. An embryonic-like methylation pattern of classical satellite DNA is observed in ICF syndrome. Hum Mol Genet. (June 1993); 2(6): 731-5.

69. Hernandez R, Frady A, Zhang XY, Varela M, Ehrlich M. Preferential induction of chromosome 1 multibranched figures and whole-arm deletions in a human pro-B cell line treated with 5-azacytidine or 5-azadeoxycytidine. Cytogenet Cell Genet. (1997); 76(3-4): 196-201.

70. Hendrickson EA. Cell-cycle regulation of mammalian DNA double-strand-break repair. Am J Hum Genet. (October 1997); 61(4): 795-800.

71. Burma S, Chen BP, Murphy M, Kurimasa A, Chen DJ. ATM phosphorylates histone H2AX in response to DNA double-strand breaks. J Biol Chem. 9 (November 2001); 276(45): 42462-7.

72. Pastwa E, Blasiak J. Non-homologous DNA end joining. Acta Biochim Pol. (2003); 50(4): 891-908.

73. Sancar A, Lindsey-Boltz LA, Unsal-Kacmaz K, Linn S. Molecular mechanisms of mammalian DNA repair and the DNA damage checkpoints. Annu Rev Biochem. (2004); 73: 39-85.

74. Allard S, Masson JY, Cote J. Chromatin remodeling and the maintenance of genome integrity. Biochim Biophys Acta. 15 (March 2004); 1677(1-3): 158-64.

75. Foster ER, Downs JA. Histone H2A phosphorylation in DNA double-strand break repair. Febs J. (July 2005); 272(13): 3231-40.

76. Li A, Eirin-Lopez JM, Ausio J. H2AX: tailoring histone H2A for chromatin-dependent genomic integrity. Biochem Cell Biol. (August 2005); 83(4): 505-15.

77. Sedelnikova OA, Pilch DR, Redon C, Bonner WM. Histone H2AX in DNA damage and repair. Cancer Biol Ther. (May-June 2003); 2(3): 233-5.

78. Celeste A, Petersen S, Romanienko PJ, Fernandez-Capetillo O, Chen HT, Sedelnikova OA, et al. Genomic instability in mice lacking histone H2AX. Science. 3 (May 2002); 296(5569): 922-7.

79. Bassing CH, Chua KF, Sekiguchi J, Suh H, Whitlow SR, Fleming JC, et al. Increased ionizing radiation sensitivity and genomic instability in the absence of histone H2AX. Proc Natl Acad Sci U S A. 11 (June 2002); 99(12): 8173-8.

80. Celeste A, Difilippantonio S, Difilippantonio MJ, Fernandez-Capetillo O, Pilch DR, Sedelnikova OA, et al. H2AX haploinsufficiency modifies genomic stability and tumor susceptibility. Cell. 8 (August 2003); 114(3): 371-83.

81. Bassing CH, Suh H, Ferguson DO, Chua KF, Manis J, Eckersdorff M, et al. Histone H2AX: a dosage-dependent suppressor of oncogenic translocations and tumors. Cell. 8 (August 2003); 114(3): 359-70.

82. Bostock CJ, Prescott DM, Kirkpatrick JB. An evaluation of the double thymidine block for synchronizing mammalian cells at the G1-S border. Exp Cell Res. (September 1971); 68(1): 163-8.

83. Sherwood SW, Schimke RT. Cell cycle analysis of apoptosis using flow cytometry. Methods Cell Biol. (1995); 46: 77-97.

84. Pietrobono R, Pomponi MG, Tabolacci E, Oostra B, Chiurazzi P, Neri G. Quantitative analysis of DNA demethylation and transcriptional reactivation of the FMR1 gene in fragile X cells treated with 5-azadeoxycytidine. Nucleic Acids Res. 15 (July 2002); 30(14): 3278-85.

85. Daniel R, Ramcharan J, Rogakou E, Taganov KD, Greger JG, Bonner W, et al. Histone H2AX is phosphorylated at sites of retroviral DNA integration but is dispensable for postintegration repair. J Biol Chem. 29 (October 2004); 279(44): 45810-4.

86. Davies HG, Small JV. Structural units in chromatin and their orientation on membranes. Nature. 23 (March 1968); 217(134): 1122-5.

87. Minucci S, Pelicci PG. Histone deacetylase inhibitors and the promise of epigenetic (and more) treatments for cancer. Nat Rev Cancer. (January 2006); 6(1): 38-51.

88. Yaneva M, Li H, Marple T, Hasty P. Non-homologous end joining, but not homologous recombination, enables survival for cells exposed to a histone deacetylase inhibitor. Nucleic Acids Res. (2005); 33(16): 5320-30.

APPENDIX

SUBMITTED ARTICLE

Endogenous DNA double-strand breaks connect global hypomethylation and genomic instability

Narisorn Kongruttanachok,[1] Wichai Pornthanakasem,[2] Wanpen Ponyeam,[2] Oranart Matangkasombut,[3] and Apiwat Mutirangura[2],*

[1]Inter-Department Program of BioMedical Sciences, Faculty of Graduate School,
[2]Molecular Biology and Genetics of Cancer Development Research Unit, Department of Anatomy, Faculty of Medicine,
[3]Department of Microbiology, Faculty of Dentistry,
Chulalongkorn University, Bangkok 10330, THAILAND

*Correspondence: mapiwat@chula.ac.th

The first two authors contributed equally and were listed alphabetically.

Running Title- Endogenous DSBs connect hypomethylation and instability

Summary

Global DNA hypomethylation is commonly observed in human cancers. In determining how this epigenetic event causes genomic instability, we discovered that endogenous DNA double-stand breaks (EDSBs) are normally hypermethylated across all cell types examined. The methylated EDSBs are retained in heterochromatin, which obstructs the early cellular DSB repair response. Trichostatin A treatment, which inhibits histone deacetylase and disrupts heterochromatin, released methylated EDSBs and increased the quantity and methylation level of γ-H2AX-bound DNA. DNA hypomethylation can therefore be linked to a high mutation rate if the early repair response of unmethylated EDSBs is error prone. We show here that down-regulation of DNA-dependent protein kinase, a requisite error-prone nonhomologous end-joining protein, increased unmethylated EDSBs. In contrast, defect in Ataxia Telangiectasia Mutated-mediated precise end-joining repair raised the level of EDSB methylation. These results suggest that unmethylated EDSB repair pathway is less precise. Consequently, spontaneous mutations are accumulated in relation to the genomic hypomethylation level.

Introduction

Global hypomethylation is one of the most common molecular events in the multistep carcinogenesis (1-3). This process leads to chromosome instability, characterized by a higher rate of chromosomal mutations and DNA deletion (4-6). The mechanism how these two phenomena are linked is not known. Studies in Wilm's tumor (7) and ICF syndrome (immunodeficiency, chromosomal instability and facial anomalies) (8), with loss-of-function mutations in the cytosine DNA methyltransferase *DNMT3B*, demonstrated the direct association between loss of DNA methylation and rearrangements in pericentromeric heterochromatin loci. Therefore, hypomethylation could lead to spontaneous mutations in cis. Moreover, DNA double-strand breaks (DSBs) are intermediate products of the global hypomethylation-related mutations although they occur spontaneously (4-6).

In 2003, Vilenchik and Knudson estimated the existence of endogenous DSBs (EDSBs) and concluded that EDSBs could account for a substantial fraction of oncogenic events in human carcinomas (9). If EDSBs do not arise uniformly or are not processed at equal rates across the genome, mutation hot spots should be present (9). Therefore, genome wide methylation depletion may cause genomic instability if DNA methylation influences EDSB processes.

In order to determine how DNA methylation affects EDSBs, we first developed a set of novel techniques to analyze the extent and methylation level of genomic EDSBs. We combined two PCR-based assays previously used in genome mapping research (10, 11). After establishing the assays, we then evaluated the relation between DNA methylation and EDSBs and their repair pathways.

Results

Detection of genomic EDSB methylation

First, we developed a new assay for the detection of EDSBs. Locus-specific EDSBs can be detected using ligation-mediated polymerase chain reaction (LMPCR), a commonly used PCR technique designed for the analysis of EDSBs during lymphoid development, such as V(D)J recombination (12) and somatic hypermutation (13). Since general EDSBs are believed to occur rarely and randomly throughout the genome (9),

repetitive sequences that widely intersperse in the human genome can be applied in a similar assay for the detection of EDSBs in their proximity, which would represent genome-wide EDSBs. Therefore, we combined LMPCR with interspersed repetitive sequence PCR (IRSPCR) (14) using the widely distributed LINE-1s (L1s) human retrotransposons (15), and called this assay L1-EDSB-LMPCR. In this assay, linker oligonucleotides are ligated to EDSBs in high molecular weight (HMW) DNA preparation and quantitatively analyzed by real-time PCR using an L1 primer and a Taqman probe complementary to the linker (Figure 1A). Significant amounts of EDSBs were detected in all tested cells (Figure 1B). This technique had minimal intra-assay variations, but a larger range of inter-assay variations (Figure 1C). The quantity of EDSBs was not related to the proportion of fragmented cells (Figure 1D). While there were positive amplifications, we were unable to detect any apoptotic fragmented DNA or cells, as determined by LMPCR ladder (16) and flow cytometry (17), respectively (data not shown). L1-EDSB levels did not differ relative to the directions of L1 primers used (Figure 1F).

Next, we developed an assay to analyze the methylation level of EDSBs. Previously, we had extensively studied methylation status of L1s in several cancers and normal tissues by PCR combined with bisulfite restriction analysis (COBRA) of L1s (COBRA-L1) (3). Treatment with bisulfite converts unmethylated cytosines, but not methylated cytosines, to uracils and then thymines after PCR, and thus generates detectable methylation-dependent changes in the restriction pattern of PCR-amplified L1 sequences. Methylation level is then calculated and presented as a percentage of total DNA. By combining L1-EDSB-LMPCR with COBRA-L1 through the treatment of linker-ligated DNA with bisulfite prior to PCR with L1 and linker primers and restriction analysis (COBRA-L1-EDSB), we can measure the methylation level of L1s adjacent to EDSBs, which reflects the methylation level of EDSBs in a genome wide fashion (Figure 2A). Matched-pair degree of methylation between L1 and L1-EDSB sequences was examined by COBRA-L1 and COBRA-L1-EDSB, respectively (Figure 2B). Similar to L1-EDSB-LMPCR, this technique had minimal intra-assay variations, but a larger range of inter-assay variations (Figure 2C).

Using L1-EDSB-LMPCR, significant amounts of EDSBs were detected in all samples from several cancer cell lines, including Daudi, Jurkat, Molt4, K562, SW480, and HeLa cells, as well as in normal cells, including sperm and white blood cells (WBCs) from several individuals (Figure 3A). Different cell types bore significantly different quantities of EDSBs with epithelial cells possessing less EDSBs than hematopoietic cells (Figure 3A). Matched-pair degree of methylation between L1 and L1-EDSB sequences was examined by COBRA-L1 and COBRA-L1-EDSB, respectively. Importantly, EDSBs were hypermethylated across all tested cells, including several cancer cell lines, sperm and WBCs (Figure 3B).

Since EDSBs were hypothesized to be preferentially produced in S phase from the conversion of single strand lesions (9), we assessed the amount of EDSBs and their methylation in several cell cycle phases, G0, G1/S, and S, in HeLa cells. As predicted, G0 bore the least EDSBs (Figure 3C). EDSBs were hypermethylated in most examined cell phases, with G0 being the most significant (Figure 3D). This result implies that hypermethylation of EDSBs is DNA replication-independent and the EDSB methylation level should not be positively influenced by the production of EDSBs during DNA replication.

Heterochromatin conceals methylated EDSBs.

Association of methylated EDSBs with heterochromatin may also obstruct DNA repair. To evaluate how methylation influences EDSB repair, we first measured the quantity and methylation status of γ-H2AX-bound DNA. γ-H2AX, the serine 139 phosphorylated form of histone H2AX, is one of the earliest DSB repair responses (18). γ-H2AX-bound DNA was obtained by chromatin immunoprecipitation (ChIP) (19) using a γ-H2AX antibody (20) and quantitated by real-time PCR with 5′L1 primers. We observed a linear correlation between the amount of precipitated DNA and the level of exposure to radiation, suggesting that the assay can quantitatively detect the level of response to radiation-induced DSBs (Figure 4A). Noteworthily, whereas leukemic cell lines possessed more L1-EDSB-LMPCR than did epithelial cells (Figure 3A), HeLa cells had more γ-H2AX-bound L1s than did Jurkat or Daudi cells (Figure 4B). This suggests that the quantity of γ-H2AX-bound L1s may be cell-type specific and inversely related to that

of L1-EDSB-LMPCR. When methylation status of γ-H2AX-bound DNA was analysed by COBRA-L1-H2AX, we found that γ-H2AX-bound DNA in all cells and most tested cell cycle phases was significantly hypomethylated relative to COBRA-L1-EDSB (Figure 4C). γ-H2AX-bound DNA in Daudi cells was also significantly more hypomethylated than genomic level as represented by COBRA-L1 (Figure 4C). These results show that γ-H2AX binding may be nonrandom with bias towards unmethylated DNA and there possibly exist methylated EDSBs free from γ-H2AX.

DNA methylation is usually associated with heterochromatin and histone deacetylation (21, 22). Furthermore, DSB repair can be regulated by histone acetylation, which can enhance phosphorylation of H2AX in the context of nucleosomes (23). We therefore hypothesized that methylated EDSBs that escape the γ-H2AX response are retained within heterochromatin. To test this hypothesis, we converted heterochromatin of HeLa cells into euchromatin with a histone deacetylase inhibitor, trichostatin A (TSA). After 2-8 hours of incubation with TSA, while LMPCR revealed no significant alteration of EDSB level, we indeed observed a significant increase in both the quantity and the methylation level of γ-H2AX-bound DNA (Figure 4D, E and F). Therefore, when TSA loosen the heterochromatin, the level of DNA breaks was not increased but the concealed methylated EDSBs were exposed to the early cellular DSB repair response.

Less precise repair of unmethylated EDSBs

Although methylated EDSBs are retained in heterochromatin, chromosome rearrangement or permanent breakage will inevitably occur if EDSBs remain through DNA replication. Since EDSBs were also detectable and hypermethylated under normal physiologic circumstances, we hypothesized that methylated EDSBs can be repaired but with a different biological pathway from unmethylated EDSBs. Homologous recombination repair (HRR) is an unlikely candidate to repair these methylated EDSBs, particularly in G0, since the presence of hypermethylated EDSBs is DNA replication-independent whereas HRR requires sister chromatids and is coordinated with DNA replication (24). Therefore, we investigate if NHEJ pathways that repair methylated and unmethylated EDSBs are distinct. NHEJ is thought to repair the majority of DSBs and involves error-prone religation of the two broken DNA ends (25). Recently, a subpathway

of precise NHEJ that can repair DSBs with high fidelity has been proposed (26, 27). While the DNA-dependent protein kinase catalytic subunit (DNA-PKcs), a phosphatidylinositol-3-kinase, is required for general NHEJ, Ataxia Telangiectasia Mutated (ATM) acts jointly with checkpoint kinase 2 and BRCA1 in controlling the fidelity of DNA end-joining by precise NHEJ (26).

We therefore analyzed EDSB methylation level in cells chemically or genetically deprived of DNA-PKcs and ATM. First, HeLa cells were incubated for 24 hours with vanillin, an inhibitor of phosphatidylinositol-3-kinases selective for DNA–PKcs (28). We observed sporadic accumulation of hypomethylated EDSBs when the DNA-PKcs-mediated repair of de novo EDSBs is inhibited (Figure 5A). On the contrary, when we genetically deprived ATM by stably transfecting siRNA, EDSB methylation levels remarkably increased (Figure 5B). Stably transfection of DNA–PKcs siRNA in HeLa cells causes down-regulation of not only DNA-PKcs but also ATM (Figure 5C) as has previously been observed (29). EDSB methylation levels of DNA-PKcs siRNA cells were significantly lower than that of ATM siRNA cells, especially in G0, as if the loss of DNA-PKcs compensated the influence of ATM deficiency on the methylation level of accumulated EDSBs (Figure 5B). These results suggest that DNA–PKcs is more important in the repair of unmethylated EDSBs whereas ATM is more important for methylated DNA.

Discussion

Differential repair of EDSBs could therefore be a concrete connection between global hypomethylation and genomic instability. This is further supported by the report by Chen and colleagues (6) that murine embryonic stem cells nullizygous for the major DNA methyltransferase (*Dnmt1*) gene exhibited global hypomethylation and significantly elevated rate of mutations with predominant small deletions, similar to NHEJ repair errors. Here, we proved that methylated EDSBs are able to avoid error-prone NHEJ repair and consequently the rate of spontaneous mutations is limited. The unmethylated EDSBs are preferentially repaired by DNA-PKcs-dependent imprecise NHEJ pathway. In contrast, the methylated EDSBs not only are retained in heterochromatin, which delays cellular repair responses, but also are repaired preferentially by ATM-dependent precise

NHEJ pathway (Figure 6A). As a result, more spontaneous mutations could arise in hypomethylated genomes (Figure 6B).

The discovery of hypermethylated EDSBs in all cell phases are not surprising. Although DSBs are hazardous to cells, leading to a complete loss of function of the broken genes and faulty DNA recombination, DSBs in methylated DNA should be less harmful because methylated genes usually have limited activity (21). In addition, usually in association with DNA methylation (22), the tightly packed structure of heterochromatin (30) may brace the broken chromosome and hide EDSB ends from random recombination. In S phase, EDSBs are still hypermethylated albeit with less significance than G0. This result implies that because DNA replication does not occur simultaneously throughout the genome, heterochromatin may still capture the broken late replicating DNA even during cell proliferation.

Nonetheless, it is surprising that the quantity of EDSBs is not directly associated with carcinogenesis but is influenced by cellular physiologic process. Here, we reported that L1-EDSB-LMPCR and γ-H2AX-bound L1s are cell type specific and inversely related. Whereas WBCs possessed more L1-EDSB-LMPCR than did epithelial cells, epithelial had more γ-H2AX-bound L1s than WBCs. Since EDSBs are concealed in heterochromatin, the higher quantity of EDSBs in WBCs may be due to their different chromatin organizations. Moreover, the level of γ-H2AX binding reflects the level of early DSB repair response, which in turn limits the level of remaining DSBs detectable by L1-EDSB-LMPCR at a given time. Nonetheless, it is interesting to explore if there are specific causes and physiologic consequences for WBCs in maintaining the higher level of methylated EDSBs.

The retention of EDSBs in heterochromatin may also help explain the antineoplastic mechanism of TSA. Histone deacetylase inhibitors have been found to induce cell cycle arrest and apoptosis in several tumors (31). Interestingly, cells chemically or genetically defective in non-homologous end-joining (NHEJ) have been found to respond hypersensitively to TSA in a dose-dependent manner (32). We showed here that TSA increased the amount of γ-H2AX-bound DNA as an early cellular DSB response. Therefore, the TSA- induced cell cycle arrest and apoptosis may be consequent cellular responses to exposed methylated EDSBs.

Genomic instability is a cardinal feature of cancer (33). Understanding the molecular mechanism would be essential for effective approach in cancer prevention (34). This study proposed that cellular response to EDSBs might be distinct from exogenous DSBs. For exogenous DSBs, H2AX phosphorylation can be coordinated interchangeably by ATM or DNA-PKcs (35, 36). Furthermore, histone acetylation by Tip60 is essential for loading of both ATM (37, 38) and DNA-PKcs (39). In contrast, this study proved that there are differential EDSB targets between ATM and DNA-PKcs depending on DNA methylation status. Better understanding of the biological process of EDSBs is crucial in identifying molecular targets to prevent hypomethylation-related spontaneous mutations that can lead to cancers.

Experimental Procedures

Cell Culture

The HeLa (cervical cancer), SW480 (colorectal adenocarcinoma), K562 (erythroleukemia), Daudi (B lymphoblast), Jurkat (T cell leukemia) and Molt4 (T lymphoblast) cell lines, were purchased from ATCC (Manassas, VA, USA). HeLa, K-562, and SW480 cells were cultured in Dulbecco's modified Eagle's medium (DMEM) (Gibco BRL, Invitrogen Corporation, Carlsbad, CA, USA), whereas Daudi, Jurkat and Molt4 cells were cultured in RPMI 1640 (Gibco), both supplemented with 10% fetal bovine serum (FBS). HeLa cells were synchronized at G0 phase by culture in serum deprivation medium, DMEM plus 0.2% FBS, for 48 h. HeLa cells in G1/S and S phase cells were synchronized by the thymidine block method, and were cultured with 2 mM thymidine (Sigma-Aldrich, St. Louis, MO, USA) to obtain cells at G1/S phase (40). To release cells into S phase, HeLa cells were washed and the medium was replaced with fresh medium. Cells were stained with propidium iodide and DNA content was measured by flow cytometry to determine the percentage of cells at different stages of the cell cycle as well as the percentage of fragmented and apoptotic cells (17). To evaluate histone hyperacetylation, HeLa cells were grown in serum deprivation medium with 100 ng/ml TSA (Sigma-Aldrich), an inhibitor of histone deacetylase. To inhibit DNA-PKcs, ATM, and both DNA-PKcs and ATM, HeLa cells were treated for 24 hours with 2.5 mM vanillin, 1-5 mM caffeine, and 40 μM LY294002 (Sigma-Aldrich), respectively. However, significant

cell proliferation inhibition and apoptosis were observed in LY294002 and caffeine experiments, respectively, which were not used in further analyses. For radiation treatment, the medium of HeLa cells was replaced with 15 ml of ice-cold medium, and cells were exposed to 0.01, 0.1, 1.0, 2.0, 10, 20, 40 and 60 Gy γ-rays at a rate of 6.22 cGy/min with a ^{60}Co source (Eldorado78).

HMW DNA preparation

To prepare HMW DNA, 5×10^5 cells were embedded in 1% low-melting-point agarose, lysed and digested in 400 μl of 1 mg/ml proteinase K, 50 mM Tris, pH 8.0, 20 mM EDTA, 1% sodium lauryl sarcosine (13). The plugs were rinsed four times in TE buffer for 20 min. To polish cohesive-end EDSBs, T4 DNA polymerase (New England Biolabs, Beverly, MA, USA) was added and later inactivated by adding EDTA to a concentration of 20 mM for 5 min followed by rinsing four times in TE buffer for 20 min. The modified LMPCR linkers were prepared from the oligonucleotides 5'-AGGTAACGAGTCAGACCACCGATCGCTCGGAAGCTTACCTCGTGGACGT-3' and 5′-ACGTCCACGAG-3′. The linkers (50 pmol) were ligated to HMW DNA using T4 DNA ligase (New England Biolabs) at 25 °C overnight. DNA was extracted from agarose plugs using a QIAquick gel extraction kit (QIAGEN, Basel, Switzerland). After extraction, 100 ng of DNA was tested for fragmentation using the LMPCR ladder technique (16). After primary polymerization at 72 °C for 1 min, 35 cycles of PCR were carried out using the linker primer 5′-AGGTAACGAGTCAGACCACCGA-3′ at 58 °C. The amplicons were electrophoresed in agarose gel to visualize apoptotic fragmented DNA ladders.

L1-EDSB-LMPCR

The quantity of L1-EDSB was measured by real-time PCR using a Lightcycler™ instrument (Roche Applied Science, Indianapolis, IN, USA) with the L1 primers 5′-CTCCCAGCGTGAGCGAC-3′ (outward) and 5′-AAGCCGGTCTGAAAAGCGCAA-3′ (inward), the linker primer, and the Taqman probe homologous to the 3′ linker sequence (6-fam) ACGTCCACGAGGTAAGCTTCCGAGCGA (tamra) (phosphate). Amplification was performed in 20 μl reactions with 0.2 mM dNTPs, 4 mM $MgCl_2$, 0.5 μM of each primer, 0.4 μM Taqman probe, 2 U of HotStarTaq (QIAGEN, Valencia, CA, USA), 1 μg/μl BSA, 1× PCR buffer and 10 ng of ligated DNA. Initial denaturation was at 95 °C for 15

min, followed by denaturation at 95 °C for 5 s, annealing at 58 °C for 5 s, extension for 2 min at 69 °C for up to 40 cycles, with quantification after the extension steps. Two types of control DNA were used. The first was a 100-bp oligonucleotide sequence with the 5′ linker sequence and 3′ homology to L1 oligonucleotide sequences. The second was DNA digested with *Eco*RV and *Alu*I and ligated to the LMPCR linkers. Ligated control DNA was subjected to real-time PCR for comparison with control oligonucleotide sequences to calculate the amount of control DNA DSBs. Because the control oligonucleotides degrade after several weeks of storage in working solution, for most experiments, the amounts of EDSBs were compared with the ligated control digested DNA and reported as L1-EDSB-LMPCR templates per ng of DNA.

COBRA-L1 and COBRA-L1-EDSB

Ligated HMW DNA was modified with bisulfite using a standard protocol (22). Bisulfite-modified DNA was recovered using a Wizard DNA clean-up kit (Promega, Madison, WI, USA) and desulfonated before PCR amplification. For COBRA-L-1, bisulfite-treated DNA was subjected to 35 cycles of PCR with two primers, B-L1-inward 5′-CGTAAGGGGTTAGGGAGTTTTT-3′ and B-L1-outward 5′-RTAAAACCCTCCRAACC AAATATAAA-3′, at an annealing temperature of 50 °C (3). Applying a hot-stop technique to prevent heteroduplex amplicons, α^{32}P-labeled-bisulfite-L1-outward oligo was added in the last PCR cycle. The amplicons were doubly digested in a 10 μl reaction volume with 2 U of *Taq* I and 8 U of *Tas* I in 1× *Taq* I buffer (MBI Fermentas, Vilnius, Lithuania) at 65 °C for 4 h. This is designed to detect unmethylated and methylated sequences of 98 and 80 bp, respectively. Digested products were then electrophoresed in 6% denaturing polyacrylamide gel. The intensity of DNA fragments was measured with a PhosphorImager using Image Quant software (Molecular Dynamics, GE Healthcare, Slough, UK). The LINE-1 methylation level was calculated as the percentage of *Taq* I intensity divided by the sum of *Taq* I- and *Tas* I-positive amplicons. For COBRA-L1-EDSB, the B-L1-inward oligo was replaced with B-LMPCR oligo, 5′-GTTTGGAAGTTTATTTTGTGGAT-3′, and 40 PCR cycles were carried out according to the same protocol. Bisulfite-treated Daudi, Jurkat and HeLa DNAs digested with *Eco*R V and *Alu* I and ligated LMPCR linker were used as positive controls to

normalize the inter-assay variation of all COBRA experiments. HeLa DNA without ligation was used as a negative control.

ChIP

The ChIP assay was performed essentially as previously described with some modifications (19, 20). Histone cross-linking to DNA was induced by adding formaldehyde directly to culture medium at a final concentration of 1%, with incubation at 37 °C for 10 min. After stopping the reaction with glycine (0.125 M final concentration) and incubation for 5 min at room temperature, adherent cells were washed twice with ice-cold PBS, and then scraped into ice-cold PBS containing Halt™ Protease Inhibitor Cocktail kit (Pierce, Rockford, IL, USA). Non-adherent cells were collected by centrifugation for 4 min at 510 g at 4 °C and washed as above. Nuclei were isolated by resuspending the cell pellet in cell lysis buffer (5 mM PIPES pH 8.0, 85 mM KCl, 0.5% Nonidet P-40, containing Halt™ Protease Inhibitor Cocktail kit) and incubated on ice for 20 min. Intact nuclei were collected by centrifugation at 3,210 g for 5 min at 4°C, resuspended in nuclear lysis buffer (1% SDS, 50 mM Tris-HCl pH 8.1, 10 mM EDTA, containing Halt™ Protease Inhibitor Cocktail kit), and incubated on ice for 10 min. Chromatin was sheared with an Ultrasonics sonicator at 30% power output for four 30 s intervals on ice to an average size of 500–1000 bp. After centrifugation at 21,720 g for 10 min at 4 °C, the chromatin solution was diluted 10-fold with dilution buffer (0.01% SDS, 1.1% Triton X-100, 1.2 mM EDTA, 16.7 mM Tris-HCl pH 8.1, 167 mM NaCl, containing Halt™ Protease Inhibitor Cocktail kit) and then precleared for 30 min at 4°C with protein G Plus-Agarose (Santa Cruz Biotechnology, Santa Cruz, CA, USA) with rotation. The agarose beads were pelleted for 1 min at 180 g and the chromatin fragments were immunoprecipitated overnight at 4 °C with Anti-phospho-Histone H2AX monoclonal antibody (Upstate, Charlottesville, VA, USA) or normal mouse IgG antibody as a negative control (Santa Cruz Biotechnology) on a rotator. Protein-DNA-antibody complexes were isolated by the addition of protein G Plus-Agarose. After 2 h, agarose beads were collected by centrifugation at 120 g for 1 min, washed once each in 500 mM, 550 mM and 600 mM high-salt wash buffers (0.1% SDS, 1% Triton X-100, 20 mM Tris-HCl pH 8, 2 mM EDTA, 500–600 mM NaCl), and twice in wash buffer (100 mM Tris-HCl pH 8, 500 mM LiCl, 1% Nonidet P-40, 1% deoxycholic acid). Complexes were

eluted with elution buffer (50 mM $NaHCO_3$, 1% SDS) for 15 min at room temperature. Cross-links were reversed by adding NaCl (200 mM final concentration) and RNA was removed by adding 10 mg/ml of RNase A, followed by incubation for 4 h at 65 °C, and then precipitated overnight with ethanol. Samples were deproteinized with proteinase K. After phenol/chloroform extraction, the DNA was precipitated with ethanol. The precipitated DNA was subjected to real-time 5´L1PCR and COBRA-L1.

Real-time 5´ L1 PCR

Quantification of the amount of immunoprecipitated DNA was carried out by real-time PCR using a QuantiTect SYBR Green PCR Kit (Qiagen, Basel, Switzerland) according to the manufacturer's instructions. Briefly, 1× QuantiTect SYBR Green PCR Master Mix, 0.2 μM forward primer (L1.2HpaIIRFLPF: 5´-CTCCCAGCGTGAGCGAC-3´), and 0.2 μM reverse primer (5´LIDSIP1st: 5´-ACTCCCTAGTGAGATGAACCCG-3´) were used for each PCR assay. The PCR program was initiated at 95°C for 15 min to activate the HotStarTaq DNA polymerase, followed by 50 thermal cycles of 15 s at 95 °C, 20 s at 57 °C and 20 s at 72 °C. A melting curve test (68 °C) was always carried out after the final reaction step to confirm that appropriate amplification products were obtained. Each sample was analyzed in triplicate PCR reactions. All reactions were run on a Lightcycler™ instrument (Roche Applied Science). DNA precipitated by Anti-phospho-Histone H2AX was 2 to 20-fold greater (average 10-fold) than DNA precipitated by normal mouse IgG antibody. One sample with less than double the amount of the mock control was excluded. The precise amount and methylation level of γ-H2AX-bound DNA were calculated from the quantity of anti-phospho-Histone H2AX minus the DNA bound in mock control IgG antibody experiments. The amount of γ-H2AX-bound DNA was estimated by relating the L1 quantity to positive control HeLa genomic DNA.

siRNA

The oligonucleotide sequences of siRNA targeting Ataxia Telangiectasia Mutated (ATM) and DNA-dependent protein kinase (DNA-PKcs) are as previously described by Zhang, et al (41) and An, et al (42), respectively. The sequences of siRNA oligonucleotides used in this study are: ATM-sense 5'-GATCCCGCACCAGTCCAGTATT

GGCTTCAAGAGAGCCAATAC TGGACTGGTGCTTTTTTGGAAA-3', ATM-antisense 5'-AGCTTTTCCAAAAAAGCACCAGTCCAGTATTGGCTCTCTTGAAGCCAATACTGGACTG GTGCGG-3'; DNA-PKcs-sense 5'-GATCCCGGGCGCTAATCGTACTGAATTCAAGAGA TTCAGTACGATTAGCGCCCTTTTTTGGAAA-3'; DNA-PKcs-antisense 5'-AGCTTTTCC AAAAAAGGGCGCTAATCGTACTGAATCTCTTGAATTCAGTACGATTAGCGCCCGG-3'; Rad51-sense 5'-GATCCCGAGCTTGACAAACTACTTCTTCAAGAG AGAAGTAGTTTGT CAAGCTCTTTTTTGGAAA-3', Rad51-antisense 5'-AGCTTT TCCAAAAAAGAGCTTGAC AAACTACTTCTCTCTTGAAGAAGTAGTTTGTCAAGCTCGG-3'.

Hind III and *BamH* I restriction sites were added at the upstream and downstream of each oligonucleotides, respectively. After annealing, these oligonucleotides were inserted into *Hind* III and *BamH* I sites of Psilencer™ 3.1 vector (Ambion, Austin, Texas, USA) to generate Psilencer siRNA vectors. All constructs were sequenced before use. The nonspecific siRNA vector from Psilencer kit was used as control. HeLa cells were plated in 60 mm dishes at a density of 8×10^5 cells per dish for 20-24 hours before transfection. Transfection with Psilencer vectors was mediated by siPORT™ *XP-1* (Ambion, Austin, Texas, USA) according to the manufacturer's instructions. Twenty-four hours after transfection, cells were maintained in conditioned DMEM medium supplemented with hygromycin B at concentration 250 µg/ml (Roche Applied Science) to screen for the stably transfected clones.

Western Blot analysis

Whole-cell lysates were resolved by SDS/PAGE and blotted to nitrocellulose membranes (Amersham Pharmacia). Antibodies used for Western blot included an anti-G3PDH antibody (Trevigen, Gaithersburg, MD, USA) as control; an antibody against acetylated-histone H4 which recognizes histone H4 acetylated at lysines 5, 8, 12 or 16 (Upstate, Charlottesville, VA, USA) for the analysis histone acetylation in TSA-treated cells; DNA-PKcs (G-4) (Santa Cruz Biotechnology, Santa Cruz, CA, USA) and ATM (2C1) (GeneTex, San Antonia, Tx, USA) for the analyses of DNA-PKcs and ATM levels, respectively, in siRNA experiments; and horseradish peroxidase (HRP)-goat anti-rabbit IgG (H+L) conjugate (Zymed® Laboratories, San Francisco, CA, USA) for GAPDH and acetylated-histone H4 and goat anti-mouse IgG-HRP sc-2005 HRP conjugated (Santa Cruz Biotechnology) for ATM and DNA-PKcs. Signals were developed by the

Supersignal west chemiluminescent substrate optimization kit (Pierce, Rockford, IL, USA).

Statistical Analyses

Statistical significance was determined according to an independent sample t-test, a paired sample *t*-test, or ANOVA using the SPSS program version 11.5 as specified.

Acknowledgements

Supported by the Thailand Research Fund and the National Center for Biotechnology and Genetic Engineering (Thailand). N.K. and Wi.P. were supported by the Royal Golden Jubilee Ph.D. grant. We thank Drs. Vitrote Sriuranpong and Kanya Suphapeetiporn, Chulalongkorn University and Dr. Man Liu, Yale University for critical review.

References

1. Feinberg AP, Vogelstein B. Hypomethylation distinguishes genes of some human cancers from their normal counterparts. Nature. 1983 Jan 6;301(5895):89-92.
2. Feinberg AP, Tycko B. The history of cancer epigenetics. Nat Rev Cancer. 2004 Feb;4(2):143-53.
3. Chalitchagorn K, Shuangshoti S, Hourpai N, Kongruttanachok N, Tangkijvanich P, Thong-ngam D, et al. Distinctive pattern of LINE-1 methylation level in normal tissues and the association with carcinogenesis. Oncogene. 2004 Nov 18;23(54):8841-6.
4. Lengauer C, Kinzler KW, Vogelstein B. DNA methylation and genetic instability in colorectal cancer cells. Proc Natl Acad Sci U S A. 1997 Mar 18;94(6):2545-50.
5. Eden A, Gaudet F, Waghmare A, Jaenisch R. Chromosomal instability and tumors promoted by DNA hypomethylation. Science. 2003 Apr 18;300(5618):455.
6. Chen RZ, Pettersson U, Beard C, Jackson-Grusby L, Jaenisch R. DNA hypomethylation leads to elevated mutation rates. Nature. 1998 Sep 3;395(6697):89-93.

7. Qu GZ, Grundy PE, Narayan A, Ehrlich M. Frequent hypomethylation in Wilms tumors of pericentromeric DNA in chromosomes 1 and 16. Cancer Genet Cytogenet. 1999 Feb;109(1):34-9.

8. Xu GL, Bestor TH, Bourc'his D, Hsieh CL, Tommerup N, Bugge M, et al. Chromosome instability and immunodeficiency syndrome caused by mutations in a DNA methyltransferase gene. Nature. 1999 Nov 11;402(6758):187-91.

9. Vilenchik MM, Knudson AG. Endogenous DNA double-strand breaks: production, fidelity of repair, and induction of cancer. Proc Natl Acad Sci U S A. 2003 Oct 28;100(22):12871-6.

10. Mutirangura A, Jayakumar A, Sutcliffe JS, Nakao M, McKinney MJ, Buiting K, et al. A complete YAC contig of the Prader-Willi/Angelman chromosome region (15q11-q13) and refined localization of the SNRPN gene. Genomics. 1993 Dec;18(3):546-52.

11. Mutirangura A, Greenberg F, Butler MG, Malcolm S, Nicholls RD, Chakravarti A, et al. Multiplex PCR of three dinucleotide repeats in the Prader-Willi/Angelman critical region (15q11-q13): molecular diagnosis and mechanism of uniparental disomy. Hum Mol Genet. 1993 Feb;2(2):143-51.

12. Schlissel M, Constantinescu A, Morrow T, Baxter M, Peng A. Double-strand signal sequence breaks in V(D)J recombination are blunt, 5'-phosphorylated, RAG-dependent, and cell cycle regulated. Genes Dev. 1993 Dec;7(12B):2520-32.

13. Papavasiliou FN, Schatz DG. Cell-cycle-regulated DNA double-stranded breaks in somatic hypermutation of immunoglobulin genes. Nature. 2000 Nov 9;408(6809):216-21.

14. Nelson DL, Ledbetter SA, Corbo L, Victoria MF, Ramirez-Solis R, Webster TD, et al. Alu polymerase chain reaction: a method for rapid isolation of human-specific sequences from complex DNA sources. Proc Natl Acad Sci U S A. 1989 Sep;86(17):6686-90.

15. Kazazian HH, Jr., Moran JV. The impact of L1 retrotransposons on the human genome. Nat Genet. 1998 May;19(1):19-24.

16. Staley K, Blaschke AJ, Chun J. Apoptotic DNA fragmentation is detected by a semi-quantitative ligation-mediated PCR of blunt DNA ends. Cell Death Differ. 1997 Jan;4(1):66-75.

17. Sherwood SW, Schimke RT. Cell cycle analysis of apoptosis using flow cytometry. Methods Cell Biol. 1995;46:77-97.

18. Rogakou EP, Pilch DR, Orr AH, Ivanova VS, Bonner WM. DNA double-stranded breaks induce histone H2AX phosphorylation on serine 139. J Biol Chem. 1998 Mar 6;273(10):5858-68.

19. Boyd KE, Farnham PJ. Coexamination of site-specific transcription factor binding and promoter activity in living cells. Mol Cell Biol. 1999 Dec;19(12):8393-9.

20. Daniel R, Ramcharan J, Rogakou E, Taganov KD, Greger JG, Bonner W, et al. Histone H2AX is phosphorylated at sites of retroviral DNA integration but is dispensable for postintegration repair. J Biol Chem. 2004 Oct 29;279(44):45810-4.

21. Fuks F. DNA methylation and histone modifications: teaming up to silence genes. Curr Opin Genet Dev. 2005 Oct;15(5):490-5.

22. Cameron EE, Bachman KE, Myohanen S, Herman JG, Baylin SB. Synergy of demethylation and histone deacetylase inhibition in the re-expression of genes silenced in cancer. Nat Genet. 1999 Jan;21(1):103-7.

23. Park EJ, Chan DW, Park JH, Oettinger MA, Kwon J. DNA-PK is activated by nucleosomes and phosphorylates H2AX within the nucleosomes in an acetylation-dependent manner. Nucleic Acids Res. 2003 Dec 1;31(23):6819-27.

24. Wyman C, Ristic D, Kanaar R. Homologous recombination-mediated double-strand break repair. DNA Repair (Amst). 2004 Aug-Sep;3(8-9):827-33.

25. Pastwa E, Blasiak J. Non-homologous DNA end joining. Acta Biochim Pol. 2003;50(4):891-908.

26. Wang HC, Chou WC, Shieh SY, Shen CY. Ataxia telangiectasia mutated and checkpoint kinase 2 regulate BRCA1 to promote the fidelity of DNA end-joining. Cancer Res. 2006 Feb 1;66(3):1391-400.

27. Durant ST, Nickoloff JA. Good timing in the cell cycle for precise DNA repair by BRCA1. Cell Cycle. 2005 Sep;4(9):1216-22.

28. Durant S, Karran P. Vanillins--a novel family of DNA-PK inhibitors. Nucleic Acids Res. 2003 Oct 1;31(19):5501-12.

29. Peng Y, Woods RG, Beamish H, Ye R, Lees-Miller SP, Lavin MF, et al. Deficiency in the catalytic subunit of DNA-dependent protein kinase causes down-regulation of ATM. Cancer Res. 2005 Mar 1;65(5):1670-7.

30. Davies HG, Small JV. Structural units in chromatin and their orientation on membranes. Nature. 1968 Mar 23;217(134):1122-5.

31. Minucci S, Pelicci PG. Histone deacetylase inhibitors and the promise of epigenetic (and more) treatments for cancer. Nat Rev Cancer. 2006 Jan;6(1):38-51.

32. Yaneva M, Li H, Marple T, Hasty P. Non-homologous end joining, but not homologous recombination, enables survival for cells exposed to a histone deacetylase inhibitor. Nucleic Acids Res. 2005;33(16):5320-30.

33. Cahill DP, Kinzler KW, Vogelstein B, Lengauer C. Genetic instability and darwinian selection in tumours. Trends Cell Biol. 1999 Dec;9(12):M57-60.

34. Sugimura T. Cancer prevention: past, present, future. Mutat Res. 1998 Jun 18;402(1-2):7-14.

35. Stiff T, O'Driscoll M, Rief N, Iwabuchi K, Lobrich M, Jeggo PA. ATM and DNA-PK function redundantly to phosphorylate H2AX after exposure to ionizing radiation. Cancer Res. 2004 Apr 1;64(7):2390-6.

36. Wang H, Wang M, Wang H, Bocker W, Iliakis G. Complex H2AX phosphorylation patterns by multiple kinases including ATM and DNA-PK in human cells exposed to ionizing radiation and treated with kinase inhibitors. J Cell Physiol. 2005 Feb;202(2):492-502.

37. Sun Y, Jiang X, Chen S, Fernandes N, Price BD. A role for the Tip60 histone acetyltransferase in the acetylation and activation of ATM. Proc Natl Acad Sci U S A. 2005 Sep 13;102(37):13182-7.

38. Murr R, Loizou JI, Yang YG, Cuenin C, Li H, Wang ZQ, et al. Histone acetylation by Trrap-Tip60 modulates loading of repair proteins and repair of DNA double-strand breaks. Nat Cell Biol. 2006 Jan;8(1):91-9.

39. Jiang X, Sun Y, Chen S, Roy K, Price BD. The FATC domains of PIKK proteins are functionally equivalent and participate in the Tip60-dependent activation of DNA-PKcs and ATM. J Biol Chem. 2006 Jun 9;281(23):15741-6.

40. Bostock CJ, Prescott DM, Kirkpatrick JB. An evaluation of the double thymidine block for synchronizing mammalian cells at the G1-S border. Exp Cell Res. 1971 Sep;68(1):163-8.

41. Zhang X, Succi J, Feng Z, Prithivirajsingh S, Story MD, Legerski RJ. Artemis is a phosphorylation target of ATM and ATR and is involved in the G2/M DNA damage checkpoint response. Mol Cell Biol. 2004 Oct;24(20):9207-20.

42. An J, Xu QZ, Sui JL, Bai B, Zhou PK. Downregulation of c-myc protein by siRNA-mediated silencing of DNA-PKcs in HeLa cells. Int J Cancer. 2005 Nov 20;117(4):531-7.

Figures and Legends

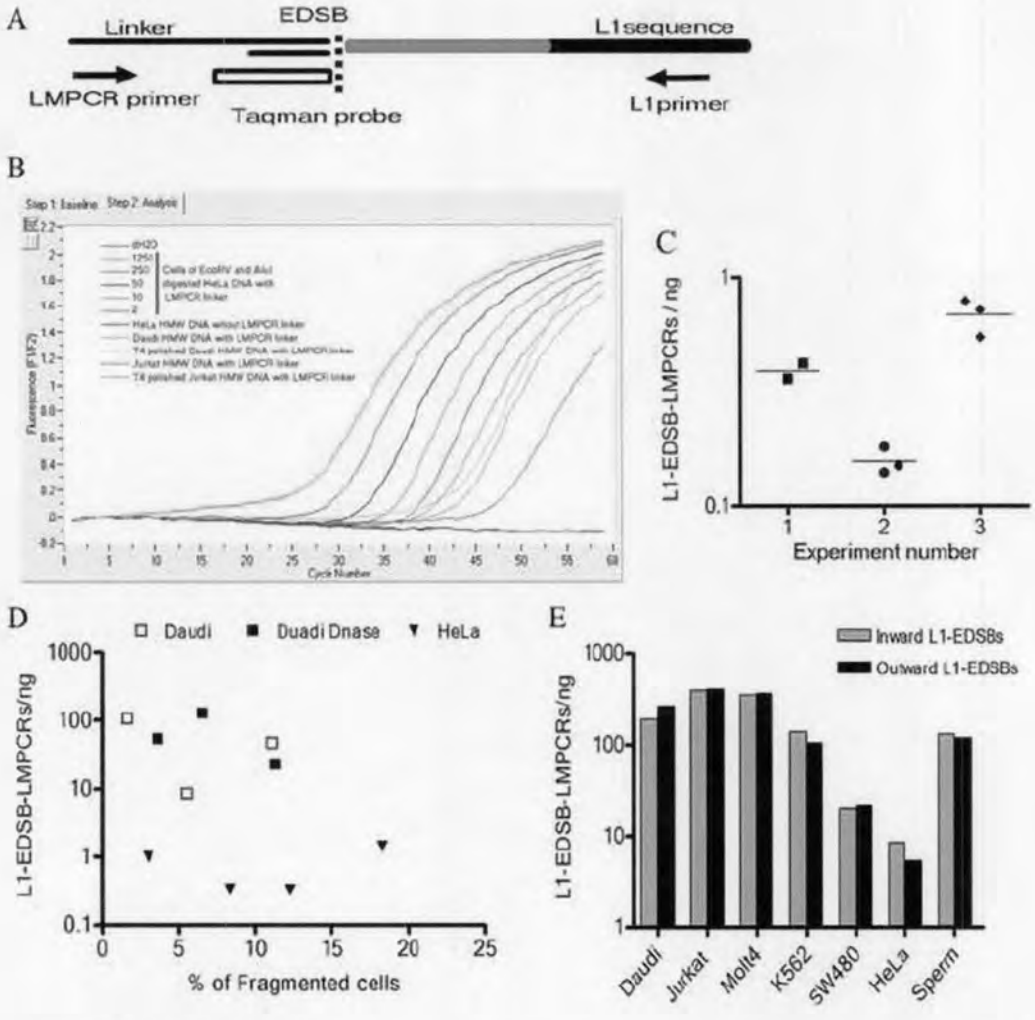

Figure 1. L1-EDSB-LMPCR

(A) Schematic representation of L1-EDSB-LMPCR showing L1 sequence ligated by linker at EDSB. The white rectangle is Taqman probe complementary to LMPCR linker. Arrows are PCR primers. (B) An example of results of real-time L1-EDSB-LMPCR with tests and controls. (C) Intra- and inter-assay variations of L1-EDSB-LMPCR. Experiment numbers 1, 2 and 3 indicate independent assays and each spot represents a different culture flask. (D) L1-EDSB-LMPCR quantity in relation to % fragmented cells, documented by flow cytometry. Daudi DNase represents Daudi cells treated with DNase I. (E) L1-EDSB-LMPCR quantities, L1 inward and outward direction. Inward L1-EDSB-LMPCR was normalized by the proportion of number of L1 oligo sequence copies in the human genome (www.ncbi.nlm.nih.gov).

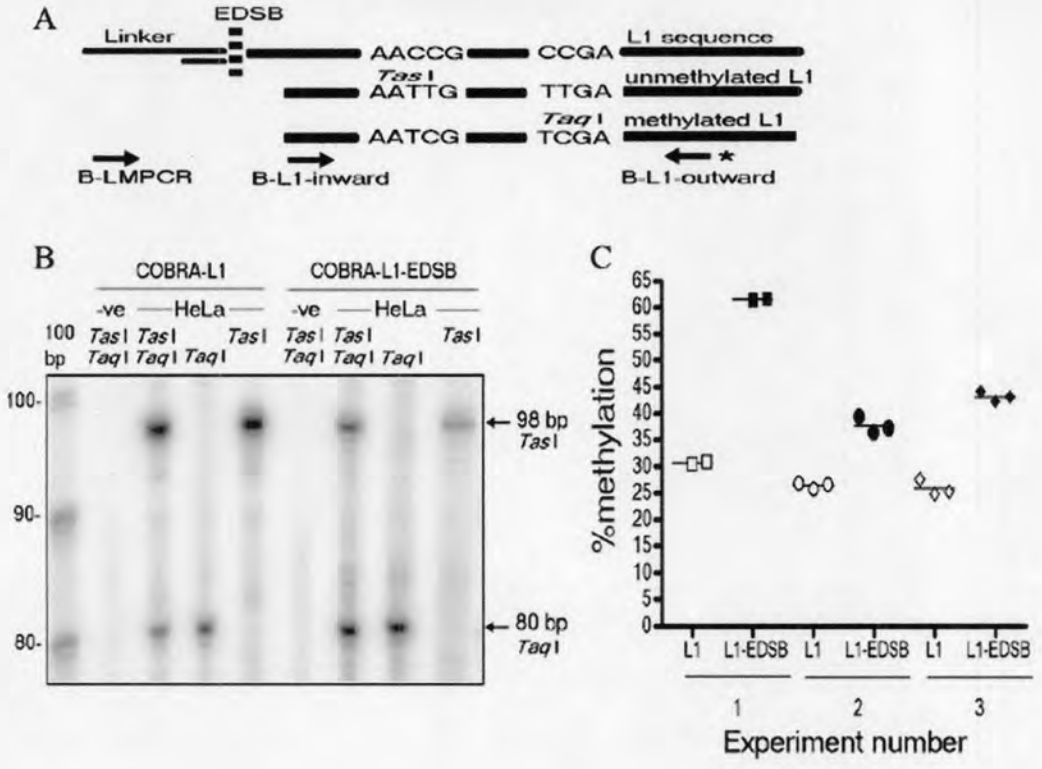

Figure 2. COBRA-L1-EDSB

(A) Schematic representation of COBRA-L1 and COBRA-L1-EDSB, showing L1 sequence ligated by linker at EDSB. Arrows are PCR primers, with star indicating α-^{32}P-labeled primer for COBRA. AACCG and CCGA are L1 sequences; when treated with bisulfite and PCR, unmethylated AACCG will be converted to AATTG (*Tas* I site) and methylated CCGA to TCGA (*Taq* I site). (B) A typical example of results from COBRA-L1 and COBRA-L1-EDSB experiments. The arrow at 98 bp indicates *Tas* I digested unmethylated L1 sequences and the arrow at 80 bp indicates *Taq* I digested methylated L1 sequences. –ve is dH2O for COBRA-L1 and nonligated HMW DNA for COBRA-L1-EDSB. *Tas* I and *Taq* I are enzymes, added in each experiment. (C) Intra- and inter-assay variations of COBRA-L1 (L1) and COBRA-L1-EDSB (L1-EDSB). Experiment numbers 1, 2 and 3 indicate independent assays and each spot represents a different culture flask.

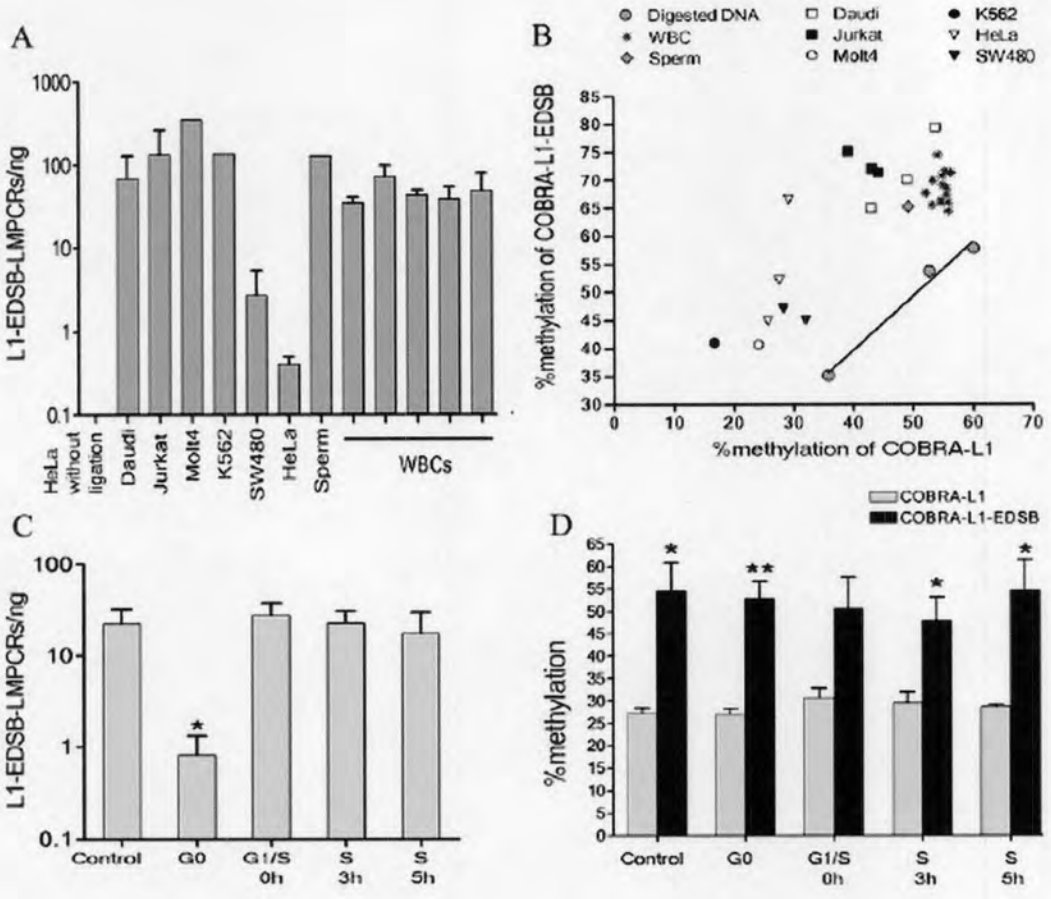

Figure 3. EDSBs are detected by L1-EDSB-LMPCR and found to be hypermethylated by COBRA-L1-EDSB.

(A) L1-EDSB-LMPCR of cancer cell lines, sperm cells, and WBCs from several individuals. (B) COBRA-L1 and COBRA-L1-EDSB comparison among cell types. Digested DNA is HeLa, Jurkat and Daudi DNA, digested with *Alu* I and *Eco*R V, as controls. (C) L1-EDSB-LMPCR and (D) COBRA-L1 and COBRA-L1-EDSB of HeLa cells at G0, G1/S, and 0, 3, and 5 h after the release into S phase from thymidine block. Control is without cell synchronization. Data represent means ±SEM. (C) **P*<0.05 (independent 1-tailed *t*-test). (D) **P*<0.05, ***P*<0.001 (pair 1-tailed *t*-test).

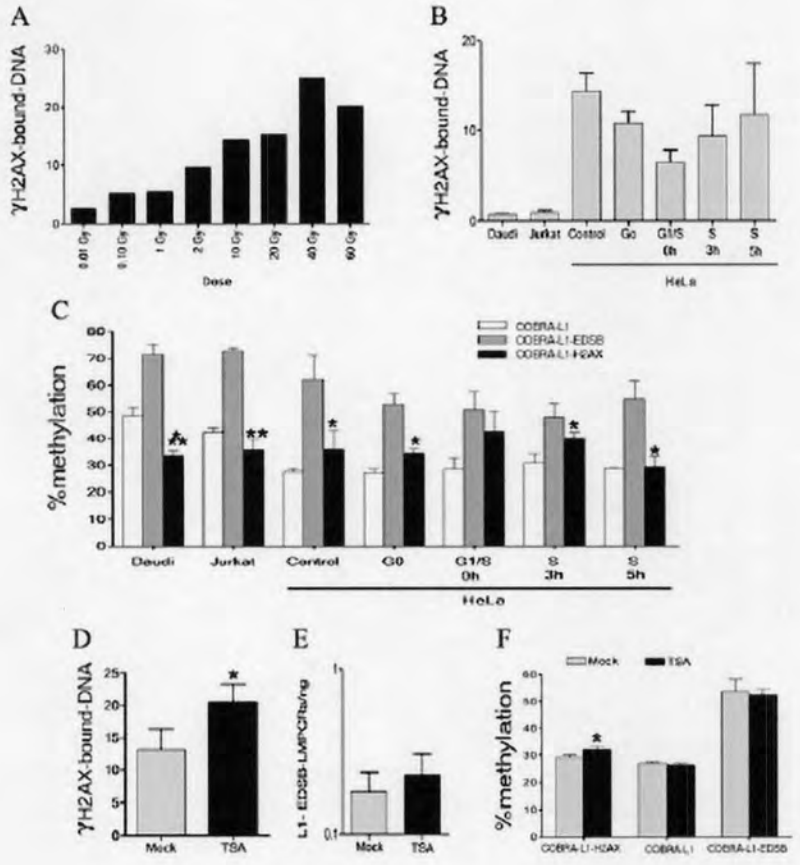

Figure 4. Methylated EDSBs are concealed from γ-H2AX in heterochromatin.

The quantity unit of γ-H2AX-bound DNA is Mb per cell. (A) γ-H2AX-bound DNA of HeLa cell in ice-cold-media after exposure to radiation. (B) γ-H2AX-bound DNA throughout the cell cycle (C) Methylation levels of different cell types and in different phases of the cell cycle. COBRA-L1-H2AX was compared with COBRA-L1-EDSB (***P<0.001, **P<0.01, *P<0.05) and with COBRA-L1 of Daudi, ***P<0.01. In (B) and (C), 0, 3, 5h are time after release into S phase. (D) Quantity of γ-H2AX-bound DNA, (E) L1-EDSB-LMPCR, and (F) comparative methylation levels of γ-H2AX-bound DNA, L1s, and EDSBs, with and without TSA. Data represent means ±SEM, with statistical significance determined by paired 1-tailed *t*-test. (E) *P<0.01 and (F) * P<0.001.

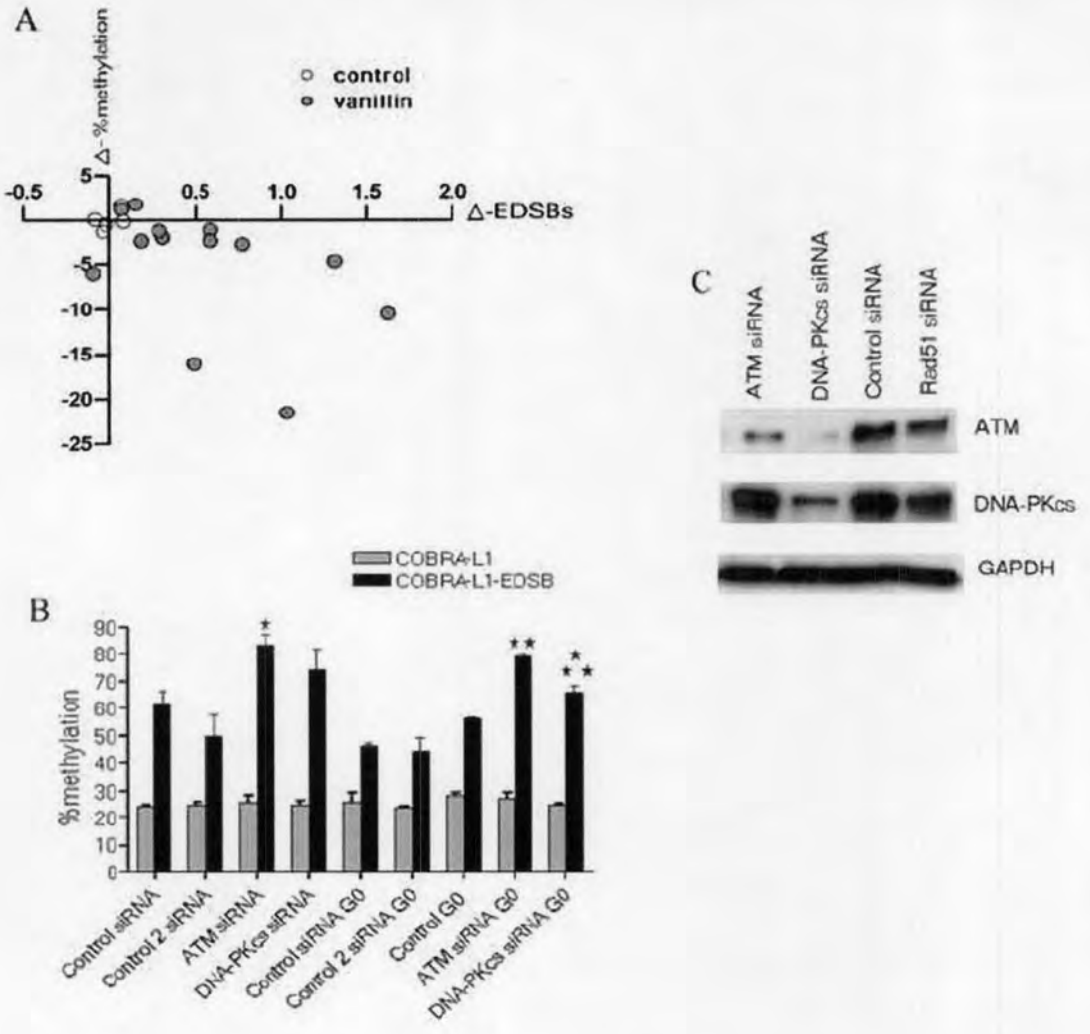

Figure 5. Inhibition of DNA-PKcs leads to accumulation of unmethylated EDSBs while down-regulation of ATM increases methylation level of EDSBs.

(A) Changes in the quantity and methylation level of EDSBs after incubation with vanillin. The Δ-EDSBs axis and the Δ-%methylation axis are values of EDSB quantity and methylation level of vanillin treated cells subtracted by the means of mock experiments, respectively. (B) COBRA-L1 and COBRA-L1-EDSB and (C) Western blotting of stable DNA-PKcs and ATM siRNA transfected HeLa cells. Control siRNA and control2 siRNA are nonspecific siRNA transfected in 2 different experiments. Control is HeLa without transfection. Data represent means ±SEM, with statistical significance determined by paired 2-tailed *t*-test, **P*<0.05, ***P*<0.001 when compared with control, and ****P*<0.01 with ATM siRNA G0.

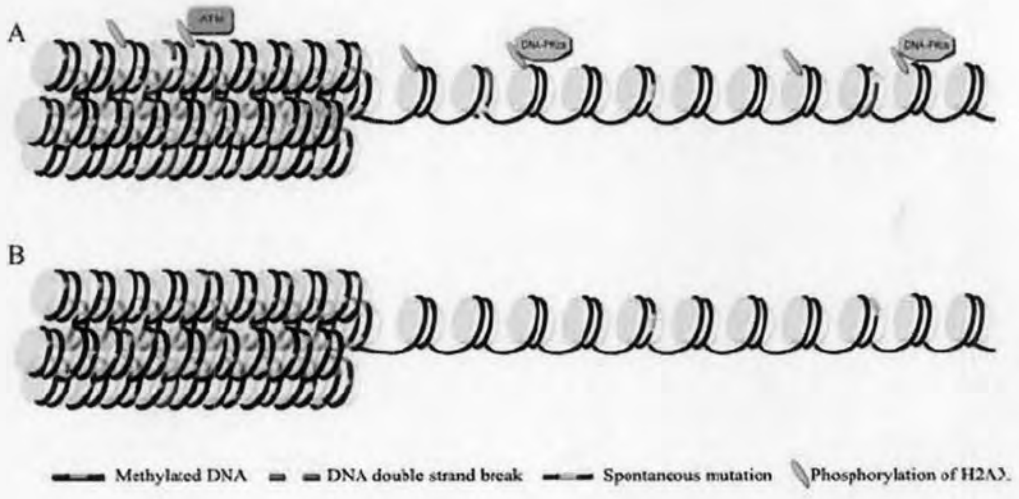

Figure 6. EDSBs are hypermethylated; methylated EDSBs are retained in heterochromatin while unmethylated EDSBs undergo less-precise repair. Diagrammatic representations of the quantity of EDSBs under normal physiologic circumstances show the differences between hyper- and hypo-methylated DNA, which associate with hetero- and eu-chromatin, respectively. (A) While methylated EDSBs are concealed in heterochromatin, the earliest DSB repair responses, γ-H2AX, are more prevalent in hypomethylated DNA. The differential nonhomologous end-joining repair pathways in nonreplicating cells between hyper and hypo-methylated DNA are shown. Whereas DNA-dependent protein kinase, a requisite error-prone nonhomologous end-joining protein, repairs unmethylated EDSBs, Ataxia Telangiectasia Mutated-mediated precise end-joining repair prefers methylated EDSBs. (B) Consequently, spontaneous mutations are accumulated in relation to the genomic hypomethylation level.

BIOGRAPHY

NAME	Miss Narisorn Kongruttanachok
DATE OF BIRTH	2nd December1975
PLACE OF BIRTH	Bangkok, Thailand
INSTITUTIONS ATTENDED	Chulalongkorn University, 1994 - 1997 Bachelor of Science (Medical Technology) Chulalongkorn University, 1998 – 2001 Master of Science (Medical Science)
RESEARCH GRANT	Royal Golden Jubilee (RGJ) Ph.D. Grant from the Thailand Research Fund (TRF)